N-Butyl Acetate Synthesis via Reactive Distillation: Thermodynamic Aspects, Reaction Kinetics, Pilot-Plant Experiments, and Simulation Studies

ARTICLE *in* INDUSTRIAL & ENGINEERING CHEMISTRY RESEARCH · OCTOBER 2002

Impact Factor: 2.59 · DOI: 10.1021/ie020179h

2 AUTHORS:

Sven Steinigeweg

7 PUBLICATIONS **317** CITATIONS

SEE PROFILE

Juergen Gmehling

Carl von Ossietzky Universität Oldenburg

382 PUBLICATIONS **11,549** CITATIONS

SEE PROFILE

n-Butyl Acetate Synthesis via Reactive Distillation: Thermodynamic Aspects, Reaction Kinetics, Pilot-Plant Experiments, and Simulation Studies

Sven Steinigeweg and Jürgen Gmehling*

Industrial Chemisty, Carl von Ossietzky University of Oldenburg, P.O. Box 2503, D-26111 Oldenburg, Germany

The development of a heterogeneously catalyzed reactive distillation process for the production of *n*-butyl acetate by the esterification of *n*-butanol with acetic acid is presented. Thermodynamic aspects of the considered system are discussed, and UNIQUAC interaction parameters are given. The reaction was catalyzed heterogeneously by a strongly acidic ion-exchange resin (Amberlyst-15). The reaction kinetics was investigated, and the kinetic constants for a pseudohomogeneous kinetic model are presented. Reactive distillation experiments were performed using the structured catalytic packing Katapak-S. Several operation conditions were varied (reboiler duty, reactant ratio, total feed rate), and two different setups were realized experimentally. The experimental results are presented in comparison with simulation results. An equilibrium stage model is capable of describing the experiments quantitatively. *n*-Butanol conversions of 98.5% accompanied with *n*-butyl acetate purities of 96.9% were achieved using an equimolar total column feed. The simulation was used subsequently to determine the influence of important design factors such as feed location, use of a prereactor, and numbers of reactive and nonreactive stages, resulting in an optimized process.

Introduction

Reactive distillation has received increasing attention over the past several years as a promising alternative to conventional processes. Especially for equilibrium-limited and consecutive reactions, reactive distillation offers distinct advantages through the direct removal of the reaction products by distillation. Therefore, conversions far beyond equilibrium conversions and higher selectivities can be obtained, leading to significantly lower investment and operating costs. Although invented in 1921,[1] the industrial application of reactive distillation did not take place before the 1980s.[2]

Especially interesting equilibrium reactions suitable for reactive distillation are esterifications, ester hydrolysis reactions, etherifications, and transesterifications. In recent years, attention has been paid to methyl acetate synthesis and hydrolysis, which serves as a model system for reactive distillation processes.[3,4]

In contrast to methyl acetate synthesis, information about *n*-butyl acetate synthesis by esterification of *n*-butanol with acetic acid (eq 1) in a reactive distillation column can hardly be found in the literature.

$$\text{acetic acid (HOAc)} + n\text{-butanol (BuOH)} \rightleftharpoons n\text{-butyl acetate (BuOAc)} + \text{water } (H_2O) \quad (1)$$

n-Butyl acetate is an important solvent in the chemical industry. Primarily it is used in paint and coating manufacture and in the lacquer industry. Because of its lower impact on the environment, *n*-butyl acetate is able to replace the toxic and teratogenic ethoxy ethyl acetate that is often used as a solvent.[5]

Investigations of different process alternatives for the production of *n*-butyl acetate have been performed by Hartig and Regner[6] and Block and Hegner.[7] These authors considered the homogeneously catalyzed reaction. Theoretical investigations of the *n*-butyl acetate system were presented by Löning et al.[8] These authors focus their attention on *n*-butyl acetate hydrolysis and analyzed reactive residue curve maps to gain insights into the different kinds of singular points present in the system. Also, data on the reaction kinetics of *n*-butyl acetate hydrolysis and the chemical equilibrium are provided, but no information about a process for the production of *n*-butyl acetate is presented. Recently, Hanika et al.[9] investigated the esterification of *n*-butanol with acetic acid by reactive distillation. These authors included only a few data about pilot-plant experiments, without supplying data on reaction kinetics. Many design strategies assume that chemical equilibrium is reached instantaneously on each reactive tray. It was shown recently by Pöpken et al.[3] that this simplification is critical for methyl acetate synthesis, and one can expect that the reaction kinetics is much more important for *n*-butyl acetate synthesis.

This paper presents a systematic approach to the development of a heterogeneously catalyzed reactive distillation process for the production of *n*-butyl acetate including reliable thermodynamic and kinetic data that cannot be found in the literature. Heterogeneously catalyzed reactive distillation offers advantages compared to homogeneous catalysis, e.g., by sulfuric acid. The size and location of the reactive section can be chosen without regard for thermodynamic constraints, and corrosion problems can be minimized. Immobilization of the heterogeneous catalyst inside the reactive section of the column can be achieved by structured

* To whom correspondence should be addressed. Tel.: +49-441-7983831. Fax: +49-441-7983330. E-mail: gmehling@tech.chem.uni-oldenburg.de. Internet: http://www.uni-oldenburg.de/tchemie/.

10.1021/ie020179h CCC: $22.00
Published on Web 10/03/2002

Table 1. Uniquac r_i and q_i Values

component	r_i	q_i
acetic acid	2.2024	2.0720
n-butanol	3.4543	3.0520
n-butyl acetate	4.8274	4.1960
water	0.9200	1.4000

packings such as Katapak-S (Sulzer Chemtech), which is used in this investigation for pilot-plant experiments. Katapak-S is made of corrugated wire-mesh sheets. Catalyst particles of 0.5 to about 2 mm can be fixed between the sheets of this packing. In this investigation, a strongly acidic ion-exchange resin (Amberlyst-15, Rohm & Haas) was used as the catalyst. Amberlyst-15 has already been applied successfully for methyl acetate synthesis and hydrolysis.[3,4] This catalyst was also employed by Löning et al.[8] for *n*-butyl acetate hydrolysis.

The procedure for the development of reactive distillation processes applied here can be divided into four steps. In the first step, the thermodynamic properties of the system are investigated to obtain a reliable description of liquid-phase nonidealities that can be used for a preliminary feasibility analysis.[10,11] Then, the reaction kinetics is investigated at conditions that are expected for the reactive distillation column. These results can be combined, and a simulation environment based on an equilibrium stage model can be employed. Experiments in a reactive distillation column on a pilot-plant scale are carried out subsequently to verify the simulation. Finally, simulation studies can be used to identify the roles of important design parameters (e.g., numbers of reactive and nonreactive stages, number and location of feed positions, role of a prereactor) and to propose an optimal setup.

Thermodynamic Aspects

The activity coefficients γ_i are necessary for the liquid-phase nonidealities to be taken into account. In this work, the UNIQUAC equation[12] was employed for the calculation of γ_i values to be used not only for the determination of phase and chemical equilibria but also for the satisfactory description of the reaction kinetics. The temperature dependence of the UNIQUAC interaction parameters was represented by polynomials of the form

$$\Delta u_{ij} = a_{ij} + b_{ij}T + c_{ij}T^2 \qquad (2)$$

Van der Waals properties *r* and *q* (Table 1) were taken from the Dortmund Data Bank (DDB), version 2002, which was kindly placed at our disposal by DDBST GmbH Oldenburg, Germany.[13] UNIQUAC interaction parameters were fitted simultaneously to the different types of phase equilibrium data [vapor−liquid equilibrium (VLE), liquid−liquid equilibrium (LLE), and azeotropic data; activity coefficients at infinite dilution (γ^∞); heats of mixing (h^E)]. Because of the complex phase equilibrium behavior with numerous azeotropes and large areas in the composition space where two liquid phases are present, only reliable and thermodynamically consistent data can be used for the determination of the UNIQUAC parameters. For the reactive systems (*n*-butanol−acetic acid, *n*-butyl acetate−water), additional VLE and h^E measurements were made by our group. These data will be published elsewhere soon. VLE measurements were performed in a static apparatus at low temperature. Heats of mixing were used to describe the temperature dependency of the activity coefficients.[14] The resulting parameters are presented in Table 2, including the parameters recently published by Horstmann et al.[14] for the system acetic acid−water. To account for the vapor-phase nonidealities, which are mainly caused by the dimerization of the carboxylic acid, the Nothnagel equation,[15] which is based on chemical theory,[16] was used.

Table 2. UNIQUAC Interaction Parameters Used for the Calculation of Activity Coefficients

component 1	component 2	*i*	*j*	a_{ij} (K)	b_{ij}	c_{ij} (K^{-1})
n-butanol	water	1	2	1783.6	−10.037	1.33×10^{-2}
		2	1	−3842.1	23.860	-3.34×10^{-2}
acetic acid	*n*-butanol	1	2	−198.40	1.563	0.0
		2	1	162.28	−1.106	0.0
n-butyl acetate	water	1	2	3512.6	−16.964	2.33×10^{-2}
		2	1	−775.4	4.448	-4.53×10^{-3}
acetic acid	*n*-butyl acetate	1	2	−61.31	−0.137	0.0
		2	1	162.09	0.279	0.0
n-butanol	*n*-butyl acetate	1	2	−48.26	0.200	-4.54×10^{-4}
		2	1	260.06	−0.499	2.12×10^{-4}
water	acetic acid	1	2	−98.12	−0.294	-7.67×10^{-5}
		2	1	422.38	−0.051	-2.40×10^{-4}

Experimental Section

Chemicals. The chemicals used for the reaction kinetics experiments were of analytical grade (99.8%, Scharlau). Water was bidistilled. For the titrimetric analysis, Titrisol (1.0 and 0.1 N sodium hydroxide, Merck) was used. The organic chemicals were dried over a molecular sieve prior to use. For the reactive distillation experiments, the chemicals were of reaction grade (99.5%) and were used without further purification. Acetic acid was supplied by Celanese, and *n*-butanol was supplied by BASF. The purity of all chemicals was verified by gas chromatography.

Analytics. All samples for reactive distillation experiments were analyzed by gas chromatography (HP 6890 instrument with TCD; He as the carrier gas at 2.4 $cm^3\ min^{-1}$; HP-Innowax 30 m × 0.032 mm column; split 10:1; temperature program = 338.15 K hold for 5 min, followed by heating at a rate of 80 K min^{-1} to 453.15 K; accuracy of mole fractions = ±0.001).

Reaction Kinetics. Löning et al.[8] presented kinetic data for the heterogeneously catalyzed hydrolysis reaction. In this article, emphasis is placed on an accurate description of the reaction kinetics of the heterogeneously catalyzed synthesis reaction. Therefore, mainly the synthesis reaction was studied. Two additional kinetic experiments were performed for the hydrolysis of *n*-butyl acetate to ensure that the kinetic constants obtained are also valid for the backward reaction.

Experiments. The experiments were conducted in a thermostated glass reactor with a volume of 500 cm^3. The temperature of the heating jacket was kept constant within ±0.1 K. The stirrer was plate-type, and the speed was variable between 100 and 800 rpm. To improve mixing, a baffle was installed. Furthermore, a reflux condenser was installed to avoid any loss of volatile components. Prior to use, the Amberlyst-15 catalyst was washed several times with water until the supernatant liquid was colorless. Before each kinetic experiment was started, both reactants were brought to reaction temperature in separate vessels. When the desired temperature was reached, the reactor was filled with both reactants and the catalyst, and time measurement was started. Liquid samples of about 1 cm^3 volume were taken using a syringe, cooled to 270 K to avoid any further reaction, and weighed (accuracy of the balance

Table 3. Kinetic Parameters for the Pseudohomogeneous Kinetic Model

reaction	i	k_i^0 (mol g^{-1} s^{-1})	$E_{A,i}$ (kJ mol^{-1})
esterification	1	6.1084×10^4	56.67
hydrolysis	−1	9.8420×10^4	67.66

= ±0.001 g). Measurements were performed in the temperature range between 331.15 and 363.15 K. In addition to the temperature of the experiments, the amount of catalyst and the initial reactant ratio were varied. Most of the experiments were continued until chemical equilibrium was reached. In all cases, the water content of the catalyst was determined after the kinetic experiment by drying the catalyst at 353 K under vacuum until the mass remained constant (usually after 2 days). The ion-exchange capacity of Amberlyst-15 was previously determined.[17]

To determine the influence of external mass transfer on the reaction rate, the stirrer speed was varied between 100 and 600 rpm in additional runs. No influence of the stirrer speed on the reaction rate was detected above 200 rpm. Therefore, further experiments were conducted at a stirrer speed of 400 rpm. Pöpken et al.[17] already showed the absence of internal mass transfer resistance for methyl acetate synthesis. Also Xu and Chuang[18] stated that internal diffusion is insignificant for the esterification of acetic acid with methanol catalyzed by Amberlyst-15. Because Amberlyst-15 is composed of very small gel-type microspheres with large macropores,[19] internal mass transfer can also be excluded for *n*-butyl acetate synthesis.

Data Analysis. Both pseudohomogeneous and adsorption-based models have been used to describe esterification reactions that are heterogeneously catalyzed by ion-exchange resins. For methyl acetate synthesis, a pseudohomogeneous model and an adsorption-based model were previously discussed,[3] and it was shown that a pseudohomogeneous model is sufficient for the description of the column profiles if small to medium amounts of water are present in the column. Esterification reactions are known to be reversible reactions of second order. Therefore, the pseudohomogeneous model can be written as

$$r = \frac{1}{m_{cat}} \frac{1}{\nu_i} \frac{dn_i}{dt} = k_1 a_{HOAc} a_{BuOH} - k_{-1} a_{BuOAc} a_{H_2O} \quad (3)$$

Activities are used instead of concentrations or mole fractions. This leads to a more consistent and accurate description.[17] The temperature dependency of the rate constant is expressed by Arrhenius' law

$$k_i = k_i^0 \exp\left(\frac{-E_{A,i}}{RT}\right) \quad (4)$$

This means that four adjustable parameters (k_1^0, k_{-1}^0, $E_{A,1}$, $E_{A,-1}$) have to be fitted for the pseudohomogeneous model. The values are given in Table 3. The Arrhenius diagram (Figure 1) shows the results from the simultaneous fit of all data at a given temperature (k_1, k_{-1}) and the result from the simultaneous fit of all experimental data available (k_1^0, k_{-1}^0, $E_{A,1}$, $E_{A,-1}$). The kinetic model (eq 3) makes the assumption of a linear relationship between the catalyst mass and the reaction rate. That this is a valid assumption can be seen from Figure 2, which shows the experimental data in comparison with calculated reaction rates.

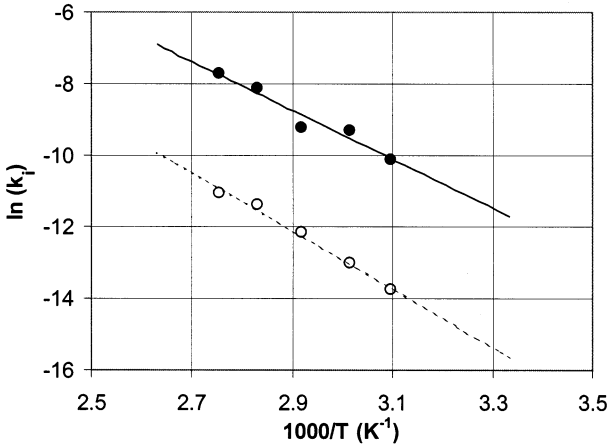

Figure 1. Arrhenius diagram of the rate constants for the esterification reaction k_1 (●) and the hydrolysis reaction k_{-1} (○) of the heterogeneously catalyzed reaction. (Lines: overall fit.)

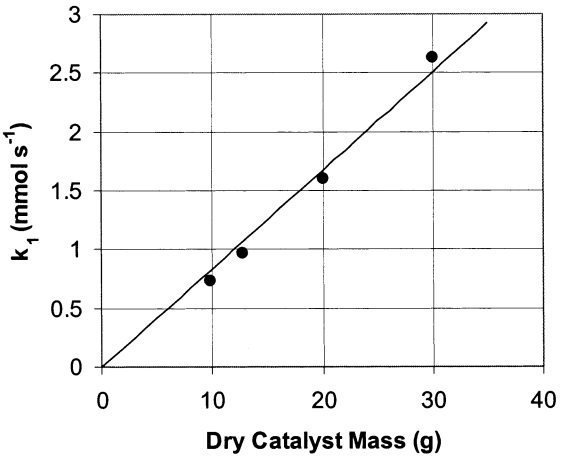

Figure 2. Rate constants for the esterification reaction k_1 (●) at 333 K versus catalyst mass. (Line: overall fit.)

Reactive Distillation Experiments. *n*-Butyl acetate, as the high-boiling product, is obtained as the bottom product. The *n*-butanol−water−*n*-butyl acetate, *n*-butanol−water, and *n*-butyl acetate−water azeotropes have similar boiling points,[20] and therefore, *n*-butanol, *n*-butyl acetate, and water are the main components present in the distillate. At higher reboiler duties, acetic acid can also be found in the distillate.

Setup. To achieve countercurrent flow in the reactive section of the column, the low-boiling reactant is usually fed into the column below the reactive section, and the high-boiling reactant is fed above the reactive section of the column. The normal boiling point of acetic acid with 391.01 K is very close to that of *n*-butanol (390.53 K), and therefore, the optimal feed locations are not obvious but an important design factor. Therefore, two different setups were employed. Figure 3 shows the first setup. For the second setup, the *n*-butanol and acetic acid feed locations were reversed. Experiments on the pilot-plant scale were performed in a glass column supplied by QVF Engineering with an inner diameter of 50 mm. A vessel with a low liquid holdup (approximately 1 dm^3) was applied as a reboiler. In the reboiler, the liquid was heated electrically by rod-shaped quartz heaters (Vogelsberger Quarzglastechnik). The reboiler duty was controlled with a transformer and determined with a digital multimeter (Voltcraft M-3860M) to within ±1%. The reactive section consisted of Katapak-S elements filled with Amberlyst-15, whereas the nonreac-

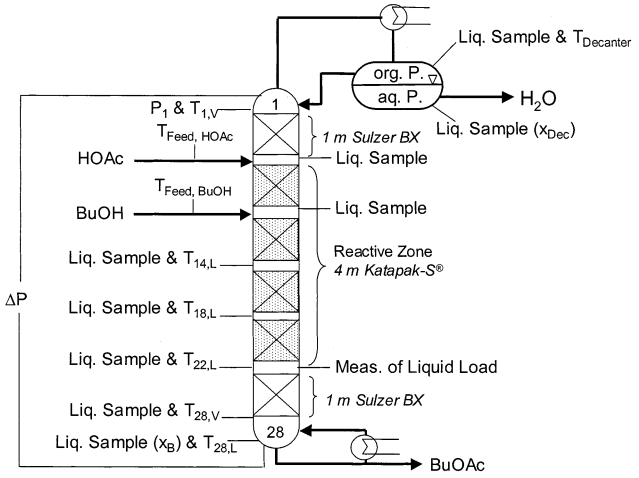

Figure 3. Setups of the reactive distillation experiments.

tive sections contained Sulzer-BX packings. Each column section had a height of 1.2 m and an effective packing height of 1 m. Except for the flanges and the reboiler, the column was insulated by a vacuum jacket. The flanges and reboiler were insulated by mineral wool. Nevertheless, the heat loss was measured previously, and a linear relationship between the temperature inside the column and the heat loss was found.[3] The heat loss was determined experimentally and can be described by the following equations

$$\dot{Q}_{\text{loss,reboiler}} = 3.8\ \text{W K}^{-1}\Delta T \qquad (5a)$$

$$\dot{Q}_{\text{loss,per section}} = 0.39\ \text{W K}^{-1}\Delta T \qquad (5b)$$

The distillate stream was condensed and collected in a decanter operated at about 359 K, which was installed at the top of the column. The aqueous phase was withdrawn, whereas the organic phase was completely refluxed into the column. All feed streams were measured by determining the mass flow using balances with an accuracy of ±1%. The column was controlled by a process control system based on Opto boards (Optoware) that were connected to a PC (WinNT workstation). Temperatures were measured using Pt-100 thermometers (accuracy of ±0.1 K). Thermometers were installed at the lower end of each column section (except at the feed positions), in the reboiler, and in the decanter. The top and bottom pressures as well as the pressure drop were recorded by pressure transducers (Bosch, accuracy ±0.1%). At the lower end of each column section, in the reboiler, and from the aqueous stream leaving the decanter, liquid samples were withdrawn by the means of a syringe, immediately cooled to 270 K to avoid any further reaction, and analyzed by gas chromatography. Below the reactive section, the liquid load of the column was measured by recording the time needed to collect a specified amount (40 cm^3) of liquid in a graduated vessel inside the column.

Experimental Results. A typical composition profile for the first setup is shown in Figure 4 and for the second setup in Figure 5. Experimental details for the first setup are given in Table 4 and for the second setup in Table 5. In this work, the aim was not only to determine the influence of relevant parameters experimentally, but also to show that it is possible to obtain high conversions accompanied by high purities of *n*-butyl acetate. As can be seen from Table 4, in experiment S1-2, *n*-butanol conversions of 98.5% in combination with *n*-butyl acetate purities of 96.9% were achieved. Figures 6 and 7 show the conversion as a function of the reboiler duty for setups 1 and 2, respectively.

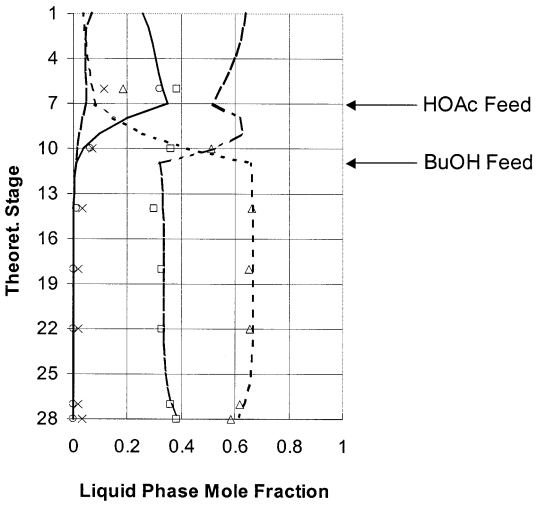

Figure 4. Profile of liquid-phase composition for S1-6. Experimental data: BuOH, △; BuOAc, □; H_2O, ×; HOAc, ○. Simulation results: BuOH, ---; BuOAc, −•−; H_2O, − −; HOAc, −.

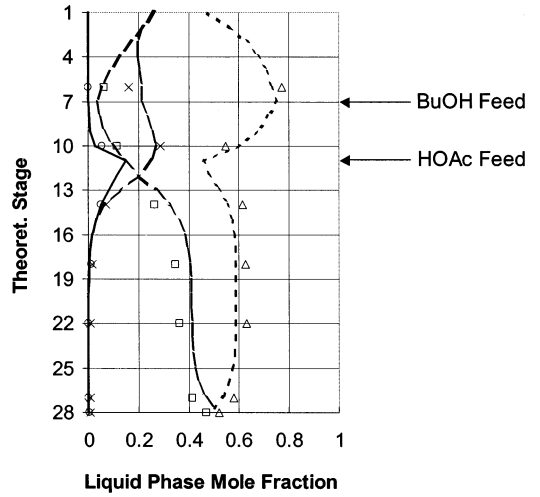

Figure 5. Profile of liquid-phase composition for S2-4. Experimental data: BuOH, △; BuOAc, □; H_2O, ×; HOAc, ○. Simulation results: BuOH, ---; BuOAc, −•−; H_2O, − −; HOAc, −.

Simulation

All simulations were carried out with the steady-state model RADFRAC from the process simulator Aspen Plus (version 10.2).[21] The model is based on a rigorous equilibrium stage model for solving the MESH equations. In addition to the UNIQUAC interaction parameters, data for the column heat loss and reaction kinetics are incorporated into the process simulator. The modeling of the decanter was achieved by the DECANTER model of Aspen Plus. For the prereactor (323.15 K), chemical equilibrium was assumed. The equilibrium constant was taken from Löning et al.[8]

The separation efficiency of Katapak-S[3] was incorporated into the simulation model without changes. For low to medium water contents, an NTSM value of 4 m^{-1} was found for Katapak-S, whereas an NTSM value of 5 m^{-1} was assumed for Sulzer-BX.[3] For the small range of liquid loads (responding to *F* factors of about 0.1−

Table 4. Experimental Data for the First Setup

run number	S1-1	S1-2	S1-3	S1-4	S1-5	S1-6	S1-7
P_1 (mbar)	995.1	1038.45	1033.84	1032.0	1028.31	1026.46	1004.79
ΔP (mbar)	4.22	20.18	4.83	2.42	3.05	7.71	7.4
$\dot{F}_{HOAc}$ (mol/h)	34.0	38.0	35.0	35.0	26.3	23	32
$\dot{F}_{BuOH}$ (mol/h)	35.0	36.0	36.0	36.0	26.5	52	40
$\dot{B}$ (mol/h)	42.0	35.0	39.0	52.0	31.9	51	44
stream leaving decanter (mol/h)	27.0	38.0	29.0	19.0	20.8	24	28
molar ratio HOAc/BuOH	0.97	1.05	1.03	0.97	0.99	0.44	0.80
x_{dec} (HOAc)	0.143	0.031	0.132	0.211	0.158	0.121	0.166
x_{dec} (BuOH)	0.000	0.008	0.003	0.002	0.004	0.006	0.002
x_{dec} (BuOAc)	0.008	0.003	0.004	0.007	0.004	0.002	0.004
x_{dec} (H_2O)	0.849	0.958	0.861	0.780	0.834	0.870	0.828
x_B (HOAc)	0.171	0.003	0.120	0.289	0.166	0.001	0.136
x_B (BuOH)	0.287	0.008	0.263	0.392	0.283	0.586	0.371
x_B (BuOAc)	0.517	0.969	0.607	0.272	0.528	0.381	0.460
x_B (H_2O)	0.025	0.020	0.010	0.047	0.023	0.031	0.033
X_{BuOH} (%)	64.58	98.5	69.42	41.56	66.33	38.09	56.47
$\dot{Q}_{reb}$ (W)	1070	2200	1150	900	850	1290	1100
w_L (m h^{-1})	9.16	14.66	8.15	4.07	6.11	9.78	9.78
$\vartheta_{feed,HOAc}$ (°C)	18.38	20.44	20.13	20.25	20.88	21.19	21.38
$\vartheta_{feed,BuOH}$ (°C)	19.31	21.94	21.44	21.38	22.19	22.56	22.69
$\vartheta_{decanter}$ (°C)	82.75	84.69	79.69	75.56	74.06	81.88	79.31
$\vartheta_{14,L}$ (°C)	93.13	118.06	95.63	96.13	95.31	117.38	94.94
$\vartheta_{28,V}$ (°C)	119.0	124.94	120.25	118.0	120.00	115.63	118.25
$\vartheta_{28,L}$ (°C)	119.75	126.13	121.06	118.0	120.88	116.63	119.13

Table 5. Experimental Data for the Second Setup

run number	S2-1	S2-2	S2-3	S2-4	S2-5
P_1 (mbar)	996.95	996.03	994.65	994.64	1002.02
ΔP (mbar)	9.16	4.59	1.56	6.44	7.72
$\dot{F}_{HOAc}$ (mol/h)	37.0	35.0	35.0	24.0	49.0
$\dot{F}_{BuOH}$ (mol/h)	36.0	36.0	36.0	47.0	24.0
$\dot{B}$ (mol/h)	37.0	42.0	54.0	46.0	49.0
stream leaving decanter (mol/h)	35.0	29.0	17.0	25.0	25.0
molar ratio HOAc/BuOH	1.03	0.97	0.97	0.51	2.04
x_{dec} (HOAc)	0.000	0.000	0.000	0.000	0.000
x_{dec} (BuOH)	0.009	0.027	0.001	0.041	0.018
x_{dec} (BuOAc)	0.001	0.008	0.000	0.009	0.001
x_{dec} (H_2O)	0.990	0.965	0.990	0.951	0.981
x_B (HOAc)	0.050	0.130	0.332	0.003	0.475
x_B (BuOH)	0.001	0.162	0.348	0.511	0.002
x_B (BuOAc)	0.930	0.629	0.307	0.476	0.474
x_B (H_2O)	0.020	0.079	0.014	0.009	0.050
X_{BuOH} (%)	98.89	77.67	48.05	45.33	98.00
$\dot{Q}_{reb}$ (W)	1340	1200	930	1200	1150
w_L (m h^{-1})	7.33	6.11	4.07	7.33	8.14
$\vartheta_{feed,HOAc}$ (°C)	19.13	20.25	20.31	20.25	20.25
$\vartheta_{feed,BuOH}$ (°C)	17.69	19.56	19.75	18.06	18.19
$\vartheta_{decanter}$ (°C)	84.63	79.65	64.13	72.63	79.75
$\vartheta_{14,L}$ (°C)	125.06	118.44	94.00	113.31	120.75
$\vartheta_{28,V}$ (°C)	123.19	123.38	111.56	115.63	119.50
$\vartheta_{28,L}$ (°C)	124.44	124.63	113.56	116.63	120.38

1.5 $Pa^{0.5}$) used during this investigation, the separation efficiency can be considered independent of the liquid load.

Stages are numbered from the top to the bottom, with stage 1 as the condenser and stage N as the reboiler. This results in 28 theoretical stages for the pilot-plant column equipped with Katapak-S (Figure 3).

Process Development

It can be seen from Figures 4−7 that the experimental data are in good agreement with the simulation results. The deviations are within experimental error for both setups. To ensure the most effective reactive distillation process, the influence of important design factors on conversion has to be evaluated. The major design parameters are the column pressure, reboiler duty, feed flow rates, number and location of feed positions, role of a prereactor, and numbers of reactive and nonreactive

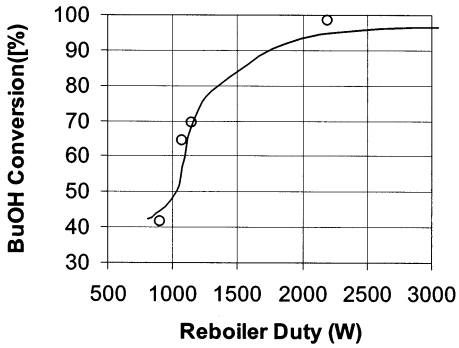

Figure 6. Conversion versus reboiler duty for setup 1. Experimental data, ○; simulation results, —.

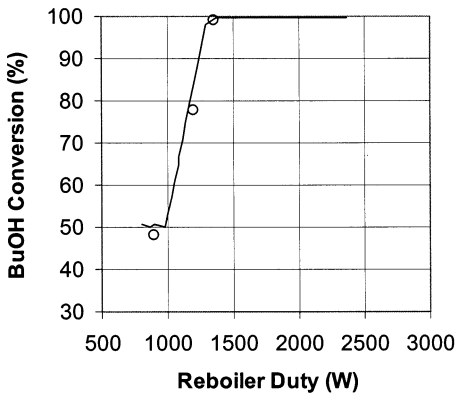

Figure 7. Conversion versus reboiler duty for setup 2. Experimental data, ○; simulation results, —.

stages. After determining the influence of these parameters, a final process can be proposed. This process can be used for a scale-up and optimization with respect to economic issues. All further calculations were conducted with the assumption of zero heat loss.

Pressure. An option to increase conversion in reactive distillation processes is to increase the column pressure and, thereby, to increase the temperature in the reactive section leading to an enhancement of the reaction rate. This is not possible using Amberlyst-15 for this reaction because the increase in the column

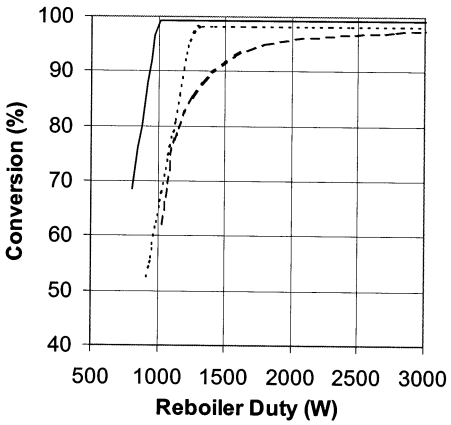

Figure 8. Conversion versus reboiler duty for different column setups. Both reactants fed above the first reactive stage (—). Acetic acid fed above the first reactive stage, *n*-butanol into the middle of the reactive section (—•—). *n*-Butanol fed above the first reactive stage, acetic acid into the middle of the reactive section (---).

pressure would result in temperatures inside the reactive section of the column that are significantly above 398 K, which is the maximum operating temperature for Amberlyst-15 recommended by the manufacturer.[19]

Reboiler Duty. It can be concluded from Figures 6 and 7 that conversions close to 100% can be obtained at high reboiler duties. The second setup experimentally investigated is more favorable because conversions close to 100% can be achieved at lower reboiler duties. Better acetic acid partitioning is achieved at lower reboiler duties in the case of the second setup.

Feed Location. The influence of the feed location on the conversion and reboiler duty is presented in Figure 8. It can be seen that the most effective approach is to feed both reactants into the column above the first reactive stage because high conversions can be expected at low reboiler duties. Feeding *n*-butanol at the top and acetic acid in the middle of the reactive section or vice versa results in higher reboiler duties necessary to obtain nearly total conversion. Feeding both reactants above the first reactive stage results in low water contents and a good distribution of the reactants in the reactive section.

Role of a Prereactor. For the prereactor, chemical equilibrium was assumed. The application of a prereactor is a favorable process alternative for minor differences in the boiling points of the reactants. Otherwise, the use of a prereactor will have a detrimental effect because both reactants are fed into the column at the same stage and countercurrent flow of the reactants in the reactive section cannot be realized. Calculations were performed with a sufficient reboiler duty that high conversions could be expected. (Usually, it was assumed that 30% of the total feed is withdrawn as bottoms.) From Figure 9, it can be concluded that the optimal feed location of the stream leaving the prereactor is above the first reactive stage. This results in an optimal distribution of the reactants in the reactive section. Feeding the prereactor stream into the column below the first reactive stage leads to a higher amount of water in the sections above the feed position and, hence, to lower conversions in these sections.

Figure 9. Conversion versus the feed location of the prereactor stream (reactive stage above which the stream is fed into the column) (equimolar feed, total feed rate of 0.14 kmol h^{-1}, 10 reactive stages, five stages each above and below reactive section).

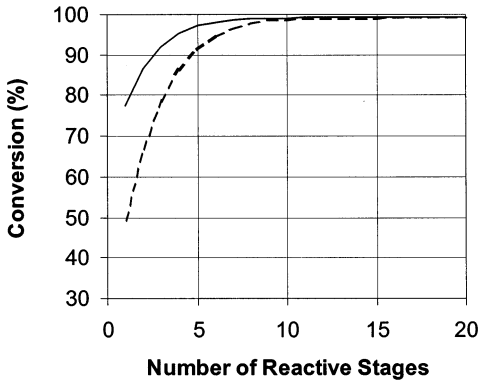

Figure 10. Conversion versus number of reactive stages (equimolar feed, total feed rate of 0.07 kmol h^{-1}, five stages each above and below reactive section). Overall conversion with (—) and without (— —) a prereactor.

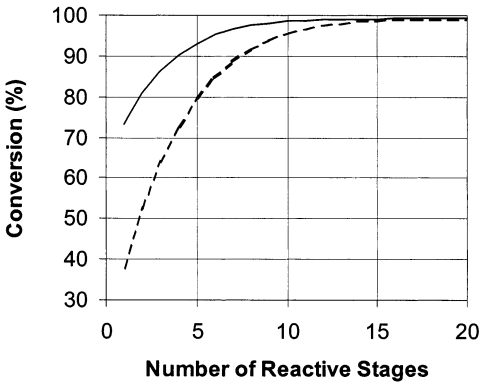

Figure 11. Conversion versus number of reactive stages (equimolar feed, total feed rate of 0.14 kmol h^{-1}, five stages each above and below reactive section). Overall conversion with (—) and without (— —) a prereactor.

Number of Reactive Stages. Figures 10 and 11 show the influence of the number of reactive stages on conversion. It can be seen that the process including the prereactor is more effective because higher conversions can be obtained for a lower number of reactive stages. For total feed rates up to 0.14 kmol h^{-1}, a minimum number of 10 reactive stages is needed. An increase in the total feed rate would demand a higher number of reactive stages. The difference between the process with and without a prereactor increases with increasing total feed flow.

Number of Nonreactive Stages. Further calculations were performed to evaluate the number of nonre-

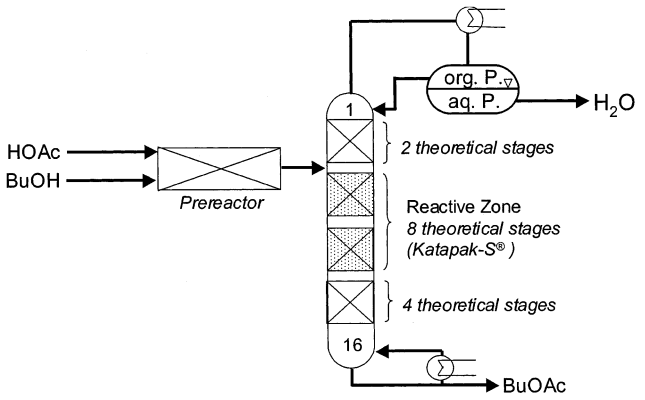

Figure 12. Scheme of the process developed (equimolar feed, total feed rate of 0.07 kmol h^{-1}).

active stages necessary. The calculations performed using a prereactor and 8 reactive stages indicate that 2 nonreactive stages above the reactive section and 4 nonreactive stages below the reactive section are necessary to achieve high conversions. Only when high-purity *n*-butyl acetate is required a higher number of nonreactive stages below the reactive section of the column is needed. The separation efficiency offered by the Katapak-S elements is sufficient for the purification of *n*-butyl acetate in the lower column sections. At the top, no further separation stages are required because the decanter ensures a sufficient separation of water from the organic compounds because of the low solubilities of *n*-butanol and *n*-butyl acetate in water.

Final Process. The previous evaluation permits us to present a process in Figure 12 that combines a minimal number of stages with high conversions and, therefore, represents a very effective manner of producing *n*-butyl acetate. A scale-up of this process to a technical plant and a further optimization with regard to economic issues is promising.

Conclusion

A procedure for the development of reactive distillation processes was applied. The thermodynamic aspects were discussed, and UNIQUAC interaction parameters were determined with the help of the Dortmund Data Bank (DDB). The reaction kinetics of *n*-butyl acetate synthesis was investigated, and kinetic constants for the pseudohomogeneous model based on activities were derived. The results were incorporated into the process simulator Aspen Plus (Aspen RADFRAC). Several reactive distillation experiments in a pilot-plant column were performed with variations in several operating conditions, including the reboiler duty, total feed flow, and reactant ratio. Furthermore, two different setups were applied. *n*-Butanol conversions of 98.5% accompanied by *n*-butyl acetate purities of 96.9% were achieved experimentally for an equimolar reactant ratio. A comparison of the experimental data with simulation results indicate that an equilibrium stage model is capable of describing the column profiles quantitatively. With the help of the reliable simulation, the influence of several important design factors was investigated. It was shown that the use of a prereactor is advantageous and that the stream leaving the prereactor should be fed into the column directly above the reaction section. The number of reactive stages necessary to achieve conversions close to 100% was determined, and the influence of the total molar feed on the number of the reactive stages was studied. It was shown that 10 reactive stages are necessary for total molar feed rates of 0.14 kmol h^{-1}. The numbers of nonreactive stages above and below the reactive section are of minor importance for the performance of the overall process. Finally, a process was proposed that can serve as the basis for the scale-up of the process and further optimization with respect to economic issues.

Acknowledgment

We thank the "Fonds der Chemischen Industrie" for providing a scholarship to S.St. and Celanese and BASF for providing the chemicals required for the measurements. Also, we express our thanks to Sulzer Chemtech for the packings. Furthermore, we thank S. Laue for performing some of the kinetic measurements.

Nomenclature

Greek Letters

γ_i = activity coefficient of component *i*
γ_i^∞ = activity coefficient at infinite dilution of component *i*
ϑ = temperature (°C)

Latin Letters

BuOAc = *n*-butyl acetate
BuOH = *n*-butanol
E_A = apparent activation energy
h^E = heat of mixing
H_2O = water
HOAc = acetic acid
k_i = kinetic constant
k_i^0 = preexponential factor
LLE = liquid−liquid equilibrium
m_{cat} = mass of catalyst
P = pressure
T = temperature
Δu_{ij} = UNIQUAC interaction parameter between components i and j
VLE = vapor−liquid equilibrium
w_L = liquid load
x_i = mole fraction
X = conversion

Subscripts

1 = esterification reaction (in kinetic expressions; otherwise, stage 1)
−1 = ester hydrolysis reaction
B = bottom stream
dec = stream leaving the decanter
i = stage number or component
L = liquid
V = vapor

Literature Cited

(1) Backhaus, A. A. Continuous Process for the Manufacture of Esters. U.S. Patent 1,400,849, 1921.

(2) Agreda, V. H.; Partin, L. R.; Heise, W. H. High-Purity Methyl Acetate via Reactive Distillation. *Chem. Eng. Prog.* **1990**, *86*, 40.

(3) Pöpken, T.; Steinigeweg, S.; Gmehling, J. Synthesis and Hydrolysis of Methyl Acetate by Reactive Distillation Using Structured Catalytic Packings: Experiments and Simulation. *Ind. Eng. Chem. Res.* **2001**, *40*, 1566.

(4) Krafczyk, J.; Gmehling, J. Einsatz von Katalysatorpackungen für die Herstellung von Methylacetat durch reaktive Rektifikation. *Chem.-Ing.-Tech.* **1994**, *66*, 1372.

(5) Kroschwitz, J. I., Ed. *Kirk-Othmer Encyclopedia of Chemical Technology. 4. Bearing Materials To Carbon*, 4th ed.; Wiley Interscience: New York, 1992; p 696.

(6) Hartig, H.; Regner, H. Verfahrenstechnische Auslegung einer Veresterungskolonne. *Chem. Ing. Technol.* **1971**, *43*, 1001.

(7) Block, U.; Hegner, B. Verfahrensvarianten eines Veresterungsverfahrens. *Verfahrenstechnik* **1977**, *11*, 157.

(8) Löning, S.; Horst, C.; Hoffmann, U. Theoretical Investigations on the Quaternary System *n*-Butanol, Butyl Acetate, Acetic Acid and Water. *Chem. Eng. Technol.* **2000**, *23*, 789.

(9) Hanika, J.; Kolena, J.; Smejkal, Q. Butyl Acetate via Reactive Distillation—Modelling and Experiment. *Chem. Eng. Sci.* **1999**, *54*, 5205.

(10) Frey, T.; Stichlmair, J. Thermodynamische Grundlagen der Reaktivdestillation *Chem. Ing. Technol.* **1998**, *70*, 1373.

(11) Bessling, B.; Löning, J.; Ohligschlaeger, A.; Schembecker, G.; Sundmacher, K. Investigations on the Synthesis of Methyl Acetate in a Heterogeneous Reactive Distillation Process. *Chem. Eng. Technol.* **1998**, *21*, 393.

(12) Abrams, D. S.; Prausnitz, J. M. Statistical Thermodynamics of Liquid Mixtures: A New Expression for the Excess Gibbs Energy of Partly or Complete Miscible Systems. *AIChE J.* **1975**, *21*, 116.

(13) *Dortmund Data Bank*; DDBST GmbH: Oldenburg, Germany, 2002 (www.ddbst.de).

(14) Horstmann, S.; Pöpken, T.; Gmehling, J. Phase Equilibria and Excess Properties for Binary Systems in Reactive Distillation Processes Part I. Methyl Acetate Synthesis. *Fluid Phase Equilib.* **2001**, *180*, 221.

(15) Nothnagel, K. H.; Abrams, D. S.; Prausnitz, J. M. Generalized Correlation for Fugacity Coefficients in Mixtures at Moderate Pressures. *Ind. Eng. Process Des. Dev.* **1973**, *12*, 25.

(16) Marek, J.; Standart, G. Vapor—Liquid Equilibria in Mixtures Containing an Associating Substance. I. Equilbrium Relationships for Systems with an Association Component. *Collect. Czech. Chem. Commun.* **1954**, *19*, 1074.

(17) Pöpken, T.; Götze, L.; Gmehling, J. Reaction Kinetics and Chemical Equilibrium of Homogeneously and Heterogeneously Catalyzed Acetic Acid Esterification with Methanol and Methyl Acetate Hydrolysis. *Ind. Eng. Chem. Res.* **2000**, *39*, 2601.

(18) Xu, Z. P.; Chuang, K. T. Effect of Internal Diffusion on Heterogeneous Catalytic Esterification of Acetic Acid. *Ind. Eng. Chem. Res.* **1997**, *52*, 33011.

(19) Pitochelli, A. R. *Ion Exchange Catalysis and Matrix Effects*; Rohm and Haas Co.: Philadelphia, PA, 1980.

(20) Gmehling, J.; Menke, J.; Krafczyk, J.; Fischer, K. *Azeotropic Data*; VCH: Weinheim, Germany, 1994.

(21) Physical Property Methods and Models. *Aspen Plus*, version 10; Aspen Technologies Inc.: Cambridge, MA, 1999.

Received for review March 7, 2002
Revised manuscript received August 22, 2002
Accepted August 28, 2002

IE020179H